AD-A239 148

(2)

REPORT DOCUMENTATION PAGE

	1b. RESTRICTIVE MARKINGS
...ICATION AUTHORITY	3. DISTRIBUTION/AVAILABILITY OF REPORT Distribution Unlimited
2b. DECLASSIFICATION/DOWNGRADING SCHEDULE	
4. PERFORMING ORGANIZATION REPORT NUMBER(S) 1991-16	5. MONITORING ORGANIZATION REPORT NUMBER(S)
6a. NAME OF PERFORMING ORGANIZATION University of Pennsylvania	6b. OFFICE SYMBOL (If applicable)
	7a. NAME OF MONITORING ORGANIZATION ONR
6c. ADDRESS (City, State, and ZIP Code) University of Pennsylvania Department of Chemistry Philadelphia, PA 19104-6323	7b. ADDRESS (City, State, and ZIP Code) 800 N. Quincy Street Arlington, VA 22217-5000
8a. NAME OF FUNDING/SPONSORING ORGANIZATION DARPA	8b. OFFICE SYMBOL (If applicable)
	9. PROCUREMENT INSTRUMENT IDENTIFICATION NUMBER
8c. ADDRESS (City, State, and ZIP Code) 3701 N. Fairfax Drive Arlington, VA 22203-1714	10. SOURCE OF FUNDING NUMBERS PROGRAM ELEMENT NO. / PROJECT NO. / TASK NO. / WORK UNIT ACCESSION NO.

11. TITLE (Include Security Classification)
"X-RAY STRUCTURE OF POLYANILINE DERIVATIVE-POLY-*ORTHO*-TOLUIDINE: THE STRUCTURAL ORIGIN OF CHARGE LOCALIZATION"

12. PERSONAL AUTHOR(S) M.E. Józefowicz, A.J. Epstein, J.P. Pouget, J.G. Masters, A. Ray and A.G. MacDiarmid

13a. TYPE OF REPORT	13b. TIME COVERED	14. DATE OF REPORT (Year, Month, Day)	15. PAGE COUNT
Technical	FROM 1-1-91 TO 10-31-91	August 7, 1991	22

16. SUPPLEMENTARY NOTATION

17. COSATI CODES			18. SUBJECT TERMS (Continue on reverse if necessary and identify by block number)
FIELD	GROUP	SUB-GROUP	polyaniline, poly-ortho-toluidine, x-ray

19. ABSTRACT (Continue on reverse if necessary and identify by block number)

We investigated the structural features of the polyaniline derivative-poly-ortho-toluidine (POT). In the base form POT is amorphous, with an x-ray diffraction pattern similar to that of emeraldine base EB-I. We estimate from the position of the broad peaks in the amorphous pattern that the interchain spacing is larger in POT-EB than in EB-I. POT hydrochloride is partially crystalline with a diffraction pattern resembling that of emeraldine hydrochloride ES-I. Analysis of the data shows that the crystalline part of POT hydrochloride adopts the ES-I like structure, with increased zig-zag angle of the polymer chain and larger interchain spacing, together with an increased disorder, possibly due to defects in the stacking of polymer chains caused by the bulky $-CH_3$ groups. Structure and percent crystallinity evolve with doping level in the same way as in the EB-I - ES-I emeraldine system. These structural results correlate with difference in the electronic properties of the POT-ES as compared with ES-I. In particular, the 10^3 decrease in room temperature conductivity of POT-ES compared to ES-I and concomitant localization of conduction electrons in POT-ES as compared with PAN-ES is attributed to the increased separation and decreased coherence between polymer chains leading to quasi-dimensional localization of conduction electrons.

20. DISTRIBUTION/AVAILABILITY OF ABSTRACT	21. ABSTRACT SECURITY CLASSIFICATION	
☒ UNCLASSIFIED/UNLIMITED ☐ SAME AS RPT. ☐ DTIC USERS	Unclassified	
22a. NAME OF RESPONSIBLE INDIVIDUAL Alan G. MacDiarmid	22b. TELEPHONE (Include Area Code) 215-898-8307	22c. OFFICE SYMBOL

DD FORM 1473, 84 MAR 83 APR edition may be used until exhausted. All other editions are obsolete.

SECURITY CLASSIFICATION OF THIS PAGE

OFFICE OF NAVAL RESEARCH

GRANT NO.: N00014-90-J-1559

R & T CODE NO.: A400004DF3

TECHNICAL REPORT NO.: 1991-16

A-1

"X-RAY STRUCTURE OF POLYANILINE DERIVATIVE-POLY-*ORTHO*-TOLUIDINE: THE STRUCTURAL ORIGIN OF CHARGE LOCALIZATION"

by

M.E. Józefowicz, A.J. Epstein, J.P. Pouget, J.G. Masters, A. Ray and A.G. MacDiarmid

Published in
Macromolecules, (In Press 1991)

University of Pennsylvania
Department of Chemistry
Philadelphia, PA 19104-6323

August 7, 1991

X-ray Structure of Polyaniline Derivative - - Poly-*ortho*-toluidine: the Structural Origin of Charge Localization.

M.E. Józefowicz[†] and A.J. Epstein[*]

Department of Physics and Department of Chemistry

The Ohio State University Columbus, Ohio 43210-1106

J.P. Pouget

Laboratoire de Physique des Solides and LURE

Université Paris-Sud, 91405 Orsay, France

J.G. Masters, A. Ray[+] and A.G. MacDiarmid

Department of Chemistry

University of Pennsylvania Philadelphia, PA 19104

June 8, 1991

Abstract

We investigate the structural features of the polyaniline derivative - poly-*ortho*-toluidine (POT). In the base form POT is amorphous, with an x-ray diffraction pattern similar to that of emeraldine base EB-I. We estimate from the position of the broad peaks in the amorphous pattern that the interchain spacing is larger in POT-EB than in EB-I . POT hydrochloride is partially crystalline with a diffraction pattern resembling that of emeraldine hydrochloride ES-I. Analysis of the data shows that the crystalline part of POT hydrochloride adopts the ES-I - like structure, with increased zig-zag angle of the polymer chain and larger interchain spacing, together with an increased disorder, possibly due to defects in the stacking of polymer chains caused by the bulky -CH_3 groups. Structure and percent crystallinity evolve with doping level in the same way as in the EB-I - ES-I emeraldine system. These structural results correlate with difference in the electronic properties of the POT-ES as compared with ES-I. In particular, the 10^3 decrease *in room* temperature conductivity of POT-ES compared to ES-I and concommittant localization of conduction electrons in POT-ES as compared with PAN-ES is attributed to the increased separation and decreased coherence between polymer chains leading to quasi-one-dimensional localisation of conduction electrons.

1 Introduction

The polyaniline family of polymers has become a prototype system for study of control of electronic phenomena due to ease of its processability and ready derivatization [1, 2, 3]. Recent studies have shown a two order of magnitude increase in conductivity of emeraldine hydrochloride (PAN-ES) with increased orientation and crystallinity [4, 5]. In contrast, extensive experiments on the methyl derivative of polyaniline, poly-*ortho*-toluidine (POT) (Fig. 1) have demonstrated that its hydrochloride salt (POT-ES) has the same electronic structure as PAN-ES yet dramatically reduced conductivity [6]. The origin of these contrasting phenomena has been proposed [6] as due to increased conduction electron localization in POT-ES as compared to PAN-ES caused by an increased interchain separation and reduced interchain order. The roles of itrachain and interchain spatial coherences have been suggested as central to the formation of the metallic state in polymers [6, 7, 8, 9]. Detailed studies of the evolution of the structures of polyanilines are therefore essential.

Fig. 1.

The crystal structure of the parent polyaniline has received substantial attention [10, 11, 12, 13]. It was shown that there were two distinct structural classes for emeraldine [11, 12]. Class I materials consisted of those prepared from solution in the conducting salt form. They have ES-I crystal structure in their ordered regions. When dedoped they form essentially amorphous EB-I. Class II materials consists of those prepared in the insulating base form. They have the EB-II crystal structure in their ordered regions and, when doped, have the ES II crystal structure. A detailed description of the differences in the ES-I and ES-II crystal structures has been earlier reported [12].

We report here the results of detailed structural study of poly-*ortho*-toluidine. We

find that POT is very similar to Class I of emeraldine in the evolution of its structure from nearly amorphous base (POT-EB) to partially crystalline HCl salt (POT-ES) on equilibration with HCl solution of appropriate pH. We have been unsuccessful at preparing a POT analogue of EB-II- and ES-II-like phases. There are significant differences between POT-EB and -ES and PAN EB-I and ES-I as well. These include an average ~4% larger interchain spacing and reduced spatial interchain coherence. These results support the thesis that the dramatic differences in transport phenomena between POT-ES and PAN-ES are due to increased localization of conduction electrons caused by reduced interchain overlap and spatial coherence.

2 Experimental Methods

Poly-*ortho*-toluidine was synthesized in the HCl salt form (POT-ES) according to the standard procedure [15], which is very much similar to the emeraldine synthesis method [3]. It was then converted to base (POT-EB) form by washing with 0.1 M NH_4OH solution. The base form was subsequently doped by equilibrating POT-EB powder with aqueous solutions of HCl of various concentration. The maximal doping level of [Cl]/[N] = 0.5 was attained by stirring POT-EB with 2.5M HCl. The [Cl]/[N] ratios (i.e., doping levels) of doped samples were determined by elemental analyses. Attempts at preparing partially crystalline POT-EB from N-methyl-2-pyrrolidone (analogous to preparation of partially crystalline EB-II) were unsuccessful.

As in our earlier studies of emeraldine system [11, 12, 14] x-ray data were collected on photographic films fixed in a cylindrical camera with the powder sample placed in a sealed Lindemann glass capillary in the center of the evacuated chamber. X-ray patterns

were taken using monochromatized CuKα (λ = 1.542Å) radiation. Additional data were also obtained with higher resolution x-ray synchrotron radiation (λ = 1.596Å) at station D-16 at LURE (Orsay). X-ray films were read in the equatorial plane using a Joyce-Loeble microdensitometer.

3 Experimental Results

A Debye-Scherrer pattern of "as prepared" POT-ES is shown on Fig. 2. This spectrum was taken with synchrotron radiation, λ = 1.596Å. It exhibits well defined reflections characteristic of crystalline order on top of a broad scattering feature from amorphous regions of the sample and the Lindemann glass sample holder. An asymetric reflection with a long tail towards larger values of 2Θ can also be seen at about 2$\Theta \sim 19°$. The d-spacings calculated from the angular positions of the reflections and the edge of this asymetric scattering for both "as prepared" POT-ES and POT-ES after dedoping and redoping to [Cl]/[N] $\sim$ 0.5 are given in Table 1. For comparison purposes, the d-spacings obtained for partially crystalline emeraldine HCl salt ES-I ([Cl]/[N] ~0.5) [12] are also presented in that table. *Fig. 2*

The rings are broader than the experimental resolution of the apparatus (FWHM $\Delta(2\Theta) \approx 0.05°$ for the x-ray synchrotron data) and from reflection broadening $\Delta(2\Theta)$ the coherence length of the crystalline order in the sample L is calculated, using the Scherrer formula [16]:

$$L = \frac{0.9\lambda}{\Delta(2\Theta)\cos\Theta} \qquad (1)$$

The L values are also given in Table 1. They are of the order of 40Å.

The sharp, crystalline rings of POT-ES disappear when the sample is dedoped, that is

converted to the base form, POT-EB. A typical Debye-Scherrer pattern of the POT-EB is shown on Fig. 3. It was taken with CuKα radiation ($\lambda = 1.542$Å). It consists mainly of one broad reflection centered around $2\Theta \sim 19°$ ($d \sim 4.75$Å) and weaker broad features at $2\Theta \sim 23°$ ($d \sim 3.9$Å) and $2\Theta \sim 44°$ ($d \sim 2.05$Å). There can also be seen a small bump at $2\Theta \sim 30°$ ($d \sim 3$Å). For reference, the scattering from an empty glass capilary is indicated. These data are summarized in Table 2, together with values obtained from emeraldine base EB-I for comparison. *Fig. 3*

POT-EB when redoped with HCl becomes partially crystalline again, with continuous evolution of the x-ray pattern with doping level. Fig. 4 shows Debye-Scherrer patterns for POT samples with doping levels from 0.0 to 0.5 . Data were taken with CuKα radiation ($\lambda = 1.542$Å). Reflections characteristic of crystalline order emerge gradually as the crystallinity of the sample increases from $\sim 0\%$ for base sample to $\sim 40 - 50\%$ for the fully doped sample. Their d-spacings shift slightly with the increased doping level, as can be seen clearly in Fig. 5. On Fig. 4 it can also be seen how, upon doping, the broad reflection in POT-EB, corresponding to $d \sim 4.75$Å$(2\Theta \sim 19°)$, transforms into the asymetric one at about the same angle in POT-ES. *Fig. 4* *Fig. 5*

Diffractometer tracings of as-prepared POT-ES (Fig. 2) and dedoped and subsequently redoped POT-ES (Fig. 4) are almost identical, showing that there is no significant degradation of the crystalline order in POT-ES upon this dedoping-doping cycle. However, the long d-spacing reflection at about 20Å ($2\Theta \sim 4.6°$, Fig. 2) has disappeared.

4 Discussion of structural data

X-ray scattering patterns and their evolution with the doping level of the POT are remarkably similar to that of the EB-I - ES-I system of polyaniline-emeraldine.

4.1 Poly-*ortho*-toluidine base

We start our analysis with the quasi-amorphous base form. When the positions of the broad features of the POT-EB are compared with data for EB-I (Table 2) it can be seen that there is an increase of d-spacing from EB-I to POT-EB, but general features of scattering patterns are similar (see Fig. 3 in [12]). We can conclude therefore that the local chain array is similar in both materials.

If we assume that the peaks in the quasi-amorphous spectra of POT-EB correspond to fundamental distances d_{110}, d_{200} and d_{020} (by analogy to EB-II), we can calculate approximate interchain lateral distances of $a \sim 7.8$Å and $b \sim 6.0$Å, which yields a cross-sectional area for two chains of $\mathcal{A} = ab = 47$Å^2. This value can be compared to 44Å^2 in EB-I and EB-II [12]. This represents ~6% increase in $\mathcal{A}$ or ~3% increase in the average POT-EB interchain distance with respect to EB. This increase is probably due to the bulky -CH_3 groups in POT.

4.2 Poly-*ortho*-toluidine hydrochloride

The main peaks in the Debye-Scherrer pattern of "as prepared" POT-ES (Table 1) can be indexed with ES-I - like pseudoorthorhombic cell, shown on Fig. 6. However, there *Fig. 6* is one additional reflection at $d \sim 20$Å which represents a doubling of the chain axis

periodicity. The c parameter, corresponding to one zigzag period of the POT chain, is 9.9Å. Comparing with c = 9.6Å for ES-I, we conclude that the C-N-C angle of POT-ES is larger. This increase is likely due to steric interactions between hydrogen and methyl groups of neighboring benzene rings. It is noted that the ~20Å reflection disappears upon dedoping and subsequent redoping. This suggests that this in-chain superlattice periodicity, which is lost upon dedoping and not regained upon redoping, could be due to the long range order in the methyl group orientation being destroyed in this process.

The interchain order is not as well defined in POT-ES as compared with ES-I. An asymetric reflection is visible where the (100) peak is anticipated. Such a feature could be explained by a broadening of the (100) reflection in directions perpendicular to a^*. In contrast the (010) and (110) reflections remain clearly defined. However, the (110) reflection is significantly broader when compared with the equivalent one in ES-I. The (010) reflection is not significantly broadened. These features, consisting mainly of the contributions of the a^* direction, correspond more likely to shear displacements (probably along a) of neighboring (a,c) planes of polymer chains in the ES-I - type structure (see Fig. 6). This could be caused by disorder in the placement of Cl^- ions due to some randomness in the position of the methyl groups caused by ring flips. When d_{010} and d_{110} distances of redoped POT-ES and ES-I are compared (Table 1) we notice that, as in the base form, the average interchain spacing is larger in POT-ES by about 5%.

Apart from the resemblance of the Debye-Scherrer patterns of "as prepared" ES-I and POT-ES, perhaps the strongest argument for the similarity of their structures is somewhat parallel evolution of their x-ray patterns (Fig. 4) and d-spacings (Fig. 5) with doping level. Figures 4 and 5 can be compared with Fig. 4 and Fig. 5, respectively, in reference [12]. In

both materials the d_{001} and d_{010} distances increase with increasing doping level whereas d_{110} decreases. However, while the d-spacings of POT-ES vary for the entire [Cl]/[N] range, it was noticed previously [12] that those of ES-I saturate above $x_c \sim 0.2 - 0.3$.

5 Implications for Electronic Phenomena

The structure of POT-EB - POT-ES system is very close to that of the EB-I - ES-I system. This similarity makes possible meaningful comparisons of electronic properties between the two. In particular, the increase of the electron localization in POT-ES [6] can be explained by the increase of the interchain spacing and of the interchain disorder reducing the rate of interchain electronic transfer and by the increase of intrachain disorder reducing the in-chain scattering time. The change of parameters is due to the presence of the bulky $-CH_3$ groups and the disorder is certainly caused by some randomness in their placement. Due to this last feature correlated disorder in the ring tilt angle and in the position of the Cl^- ions will also be present.

As discussed in the introduction, though the electronic structure of POT-ES and PAN-ES appear nearly identical, their transport properties are dramatically different with POT-ES having one-dimensional localization [6] and PAN-ES showing features of three-dimensional delocalization [17]. The direct similarity of the ES-I and POT-ES structures allows conclusions to be drawn concerning the criteria for truly metallic polymers. POT-ES structure differs from that of PAN-ES-I only in terms of a ~5% increased interchain separation and reduced interchain order. This lends strong support for the critical role of the relative size of the interchain conduction electron transition rate as compared with intrachain scattering rate. The improved order and decreased interchain separation of

PAN-ES-I with respect to POT-ES is sufficient to take the former polymer to the edge of three-dimensional delocalization within crystalline regions while POT-ES remains one-dimensionally localized. It is noted that similar criteria for three-dimensional delocalization to achieve the highly conducting metallic state apply to other polymers including polyacetylene, where recent magnetoresistance studies [18] demonstrate that the conduction electrons are only weakly localized. It was also proposed [19] that, correlated with simultaneous changes of d-spacings and transverse diffusion coefficient of the carriers with x, ES-I undergoes a localization-delocalization electronic transition at about x_c.

6 Conclusions

The POT-EB - POT-ES system is structurally similar with EB-I - ES-I. This similarity makes possible meaningful comparisons of transport and other properties [6, 17]. In particular, the increased electron localization in POT-ES can be explained by increased interchain spacing and increased interchain disorder in poly-*ortho*-toluidine.

7 Acknowledgement

This work was supported in part by the Defense Advanced Research Project Agency through a contract monitored by the U.S. Office of Naval Research. Laboratoire de Physique des Solides, Laboratoire No.2 is affiliated with the Centre National de la Recherche Scientifique.

References

[†] Chemical Physics Program, The Ohio State University, Columbus, Ohio 43210-1106

[+] Present address: Alchemi Research Centre, Naharashtra, India.

[1] See, for example, Proceedings of International Conferences on Science and Technology of Synthetic Metals; Tubingen, Germany, 2-8 Sept. 1990 (*Synth. Met.* **1991**, in press); Santa Fe, N.M., 27 June - 2 July 1988 (*Synth. Met.* **1989**, *27-29*).

[2] Epstein, A.J.; MacDiarmid, A.G.; *Mat. Res. Soc. Symp. Proc.* **1990**, *173*, 293.

[3] MacDiarmid, A.G.; Epstein, A.J. *Chem. Soc. Faraday Disc.* **1989**, *88*, 317.

[4] Cromack, K.R.; Józefowicz, M.E.; Ginder, J.M.; McCall, R.P.; Du, G.; Leng, J.M.; Kim, K.; Li, C.; Wang, Z.; Epstein, A.J.; Druy, M.A.; Glatkowski, P.J.; Scherr, E.M.; MacDiarmid, A.G. *Macromolecules* **1991**, *zz*, xxx.

[5] Scherr, E.M.; MacDiarmid, A.G.; Manohar, S.K.; Masters, J.G.; Sun, Y.; Tang, X.; Druy, M.A.; Glatkowski, P.J.; Cajibe, V; Fischer, J.E.; Cromack, K.R.; Józefowicz, M.E.; Ginder, J.M.; McCall, R.P.; Epstein, A.J. *Synth. Met.* **1991**, *41*, 735.

[6] Wang, Z.H.; Javadi, H.H.S; Ray, A.; MacDiarmid, A.G.; Epstein, A.J.; *Phys. Rev. B* **1990**, *42*, 5411; Wang, Z.H.; Ray, A.; MacDiarmid, A.G.; Epstein, A.J.; *Phys. Rev. B.* **1991**, *43*, 4373.

[7] Gogolin, A.A; *Phys. Rept.* **1982**, *1*, 1; **1988** *5*, 269.

[8] Firsov, Y.A.; in *Localization and Metal-Insulator Transitions*, Fritzche, H. and Adler, D. (eds.), Plenum Press, 1955, p.477.

[9] Kivelson, S; Heeger, A.J.; *Synth. Met.* **1988**, *22*, 371.

[10] Fosong, W.; Jinsong, T.; Lixiang, W.; Hongfang, Z.; Zhishen, M.; *Mol. Cryst. Liq. Cryst.* **1988**, *160*, 175.

[11] Józefowicz, M.E.; Laversanne, R.; Javadi, H.H.S.; Epstein, A.J.; Pouget, J.P.; Tang, X.; MacDiarmid, A.G.; *Phys. Rev. B* **1989**, *39*, 12958.

[12] Pouget, J.P.; Józefowicz, M.E.; Epstein, A.J.; Tang, X.; MacDiarmid, A.G.; *Macromolecules* **1991**, *24*, 779.

[13] Moon, Y.B.; Cao, Y.; Smith, P.; Heeger, A.J.; *Polymer Comm.* **1989**, *30* 196.

[14] Józefowicz, M.E.; Epstein, A.J.; Pouget, J.-P.; Masters, J.G.; Ray, A.; Sun, Y.; Tang, X.; MacDiarmid, A.G. *Synth. Met.* **1991**, *41*, 723.

[15] Wei, Y.; Focke, W.W.; Wnek, G.E.; Ray, A.; MacDiarmid, A.G.; *J. Phys. Chem.* **1989**, *93*, 495.

[16] Guinier, A., *X-ray Diffraction in Crystals, Imperfect Crystals and Amorphous Bodies*, W.H. Freeman, San Francisco (1963)

[17] Wang, Z.H.; Li, C.; Scherr, E.M.; MacDiarmid, A.G.; Epstein, A.J; *Phys. Rev. Lett.* **1991**, *66*, 1745.

[18] Javadi, H.H.S.; Chakraborty, A.; Li, C.; Theophilou, N.; Swanson, D.B.; MacDiarmid, A.G.; Epstein, A.J.; *Phys. Rev. B* **1991**, *43*, 2183.

[19] Epstein, A.J.; MacDiarmid, A.G.; Pouget, J.P.; *Phys. Rev. Lett.* **1990**, *65*, 664.

8 Figure captions

Figure 1 Schematic formula of I) POT-EB and II) POT-ES. Due to ring torsional motion about the N-N axis, there are two possible locations for the methyl group [(a) and (b)] on each benzene ring.

Figure 2 X-ray Debye-Scherrer pattern from "as prepared" poly-*ortho*-toluidine hydrochloride, taken at LURE (λ = 1.596Å). Dashed line shows contribution from glass sample holder.

Figure 3 X-ray Debye-Scherrer pattern from poly-*ortho*-toluidine base (λ = 1.542Å). Dashed line shows contribution from glass sample holder.

Figure 4 Set of microdensitometer readings of x-ray Debye-Scherrer patterns showing the continous evolution from POT-EB to POT-ES as a function of the [Cl]/[N] ratio (λ = 1.542Å). The various tracings are not scaled to each other.

Figure 5 Variation of the d-spacing of the (001), (010) and (110) reflections (from top to bottom) of POT-ES as a function of the doping level ([Cl]/[N] ratio).

Figure 6 Projection along the chain axis and side view of the ES-I pseudo-orthorhombic unit cell (from [12]). Black rectangles on the upper drawing represent projections of polymer chains on the (*a*,*b*) plane. Zigzags on the lower part represent schematic view of the polymer chain. Circles denote Cl^- ion.

Table 1 *d*-spacing, coherence length L and intensity corresponding to crystalline reflections of POT-ES "as prepared" and redoped to [Cl]/[N] $\sim$ 0.5. For comparison, the ES-I data of Ref. [12] and (hkl) indexing with a pseudoorthorhombic structure are

given. The d-spacing of assymetric reflections ($^+$) corresponds to the low 2Θ edge of scattering.

Table 2 d-spacing corresponding to broad peaks and a bump ($\sim$) observed in the x-ray patterns of POT-EB and EB-I. The (hkl) indexing refers to the EB-II structure defined in ref.[12].

TABLE 1

d-spacing (L) [Å]						(hkl)
POT-ES as prepared		POT-ES redoped		ES-I (from [12])		
~20 (60)	w					
9.95 (40)	s	9.85 (35)	s	9.57 (45)	s	(001)
6.5 (35)	m	6.4 (35)	m	5.94 (35)	s	(010)
~4.7+		~4.7+		4.26 (35)	s	(100)
3.61 (40)	s	3.61 (35)	s	3.51 (70)	vs	(110)
3.38	w	3.36	w	3.28	m	(111)
~3.25	vw	3.23	vw	2.98	w	(020)
~3.03	vw	~3.03	vw	2.85	vw	(021)
~2.45	vw	~2.42	vw	2.47	vw	
				2.34	vw	
~2.10	vw	~2.08	vw	2.10	vw	
				1.72	vw	

TABLE 2

d-spacing [Å]		(hkl)
POT-EB	EB-I	
4.75	4.45	(110)
3.9	~ 3.75	(200)
~3.0	2.95	(020)
2.05	2.02	

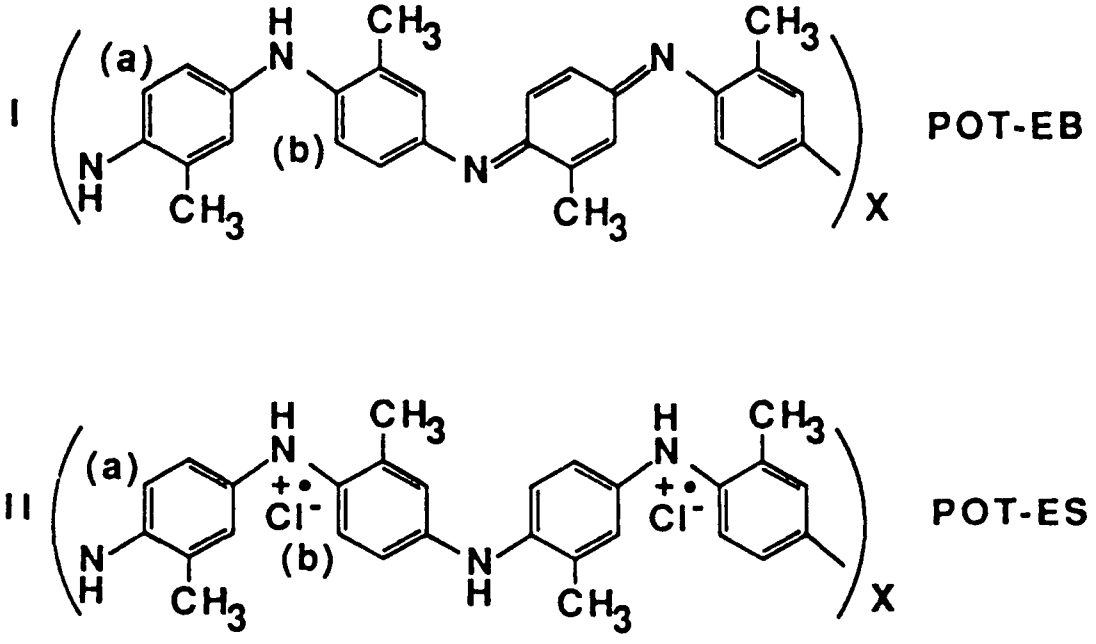

Jozefowicz et al. Figure 1

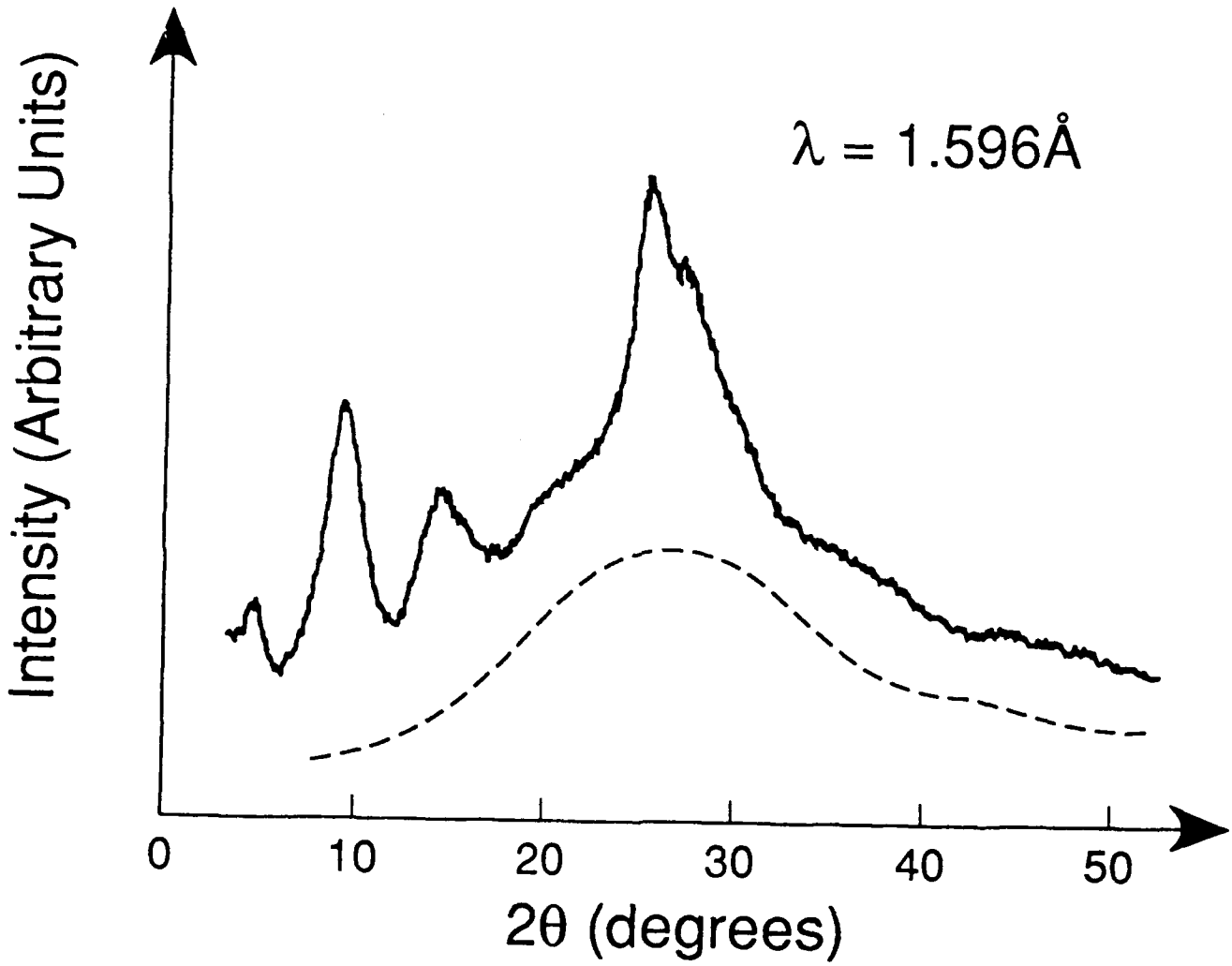

Jozefowicz et al. Figure 2

F2/51-38/1

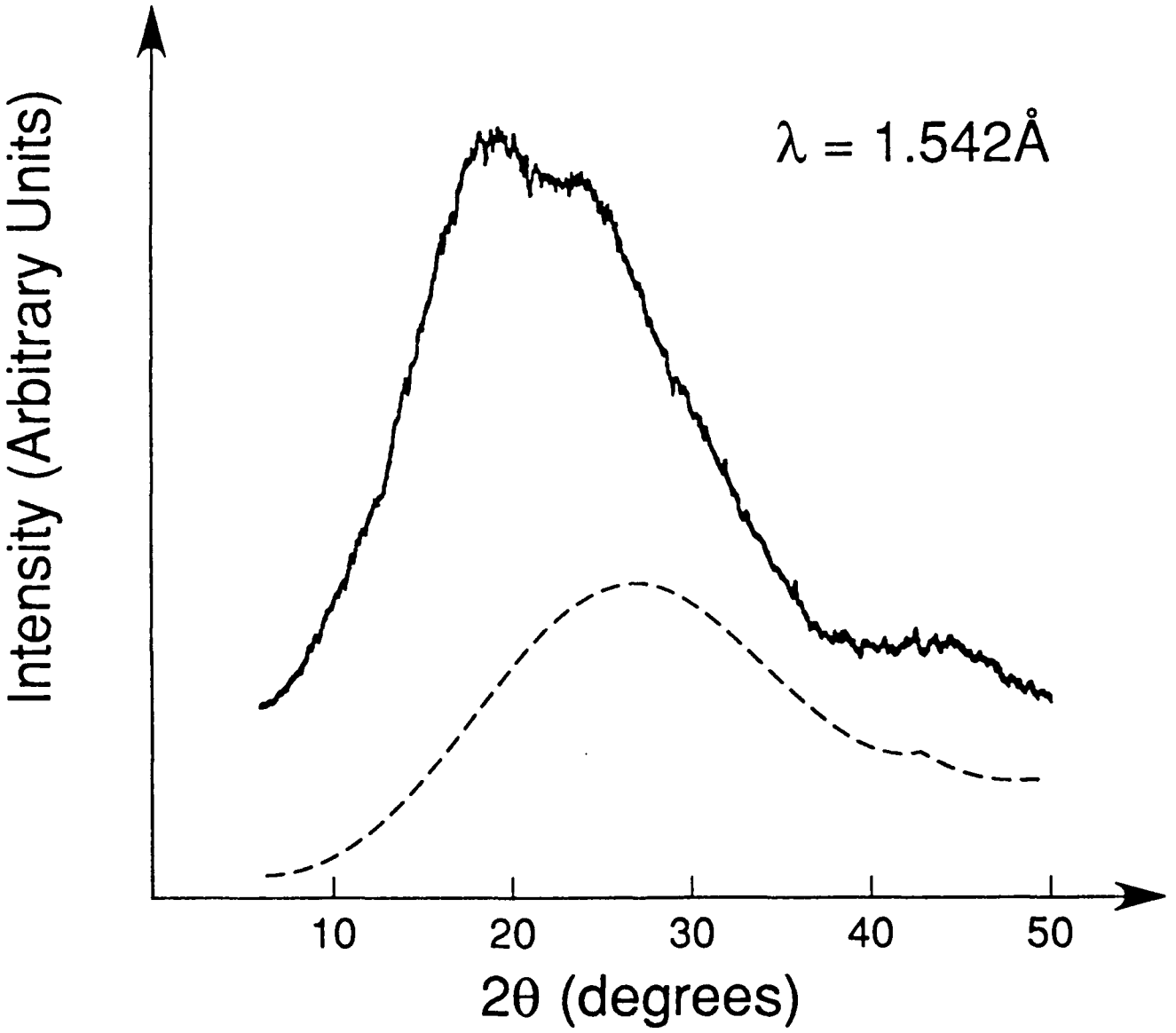

Jozefowicz et al. Figure 3

F2/51-38/2

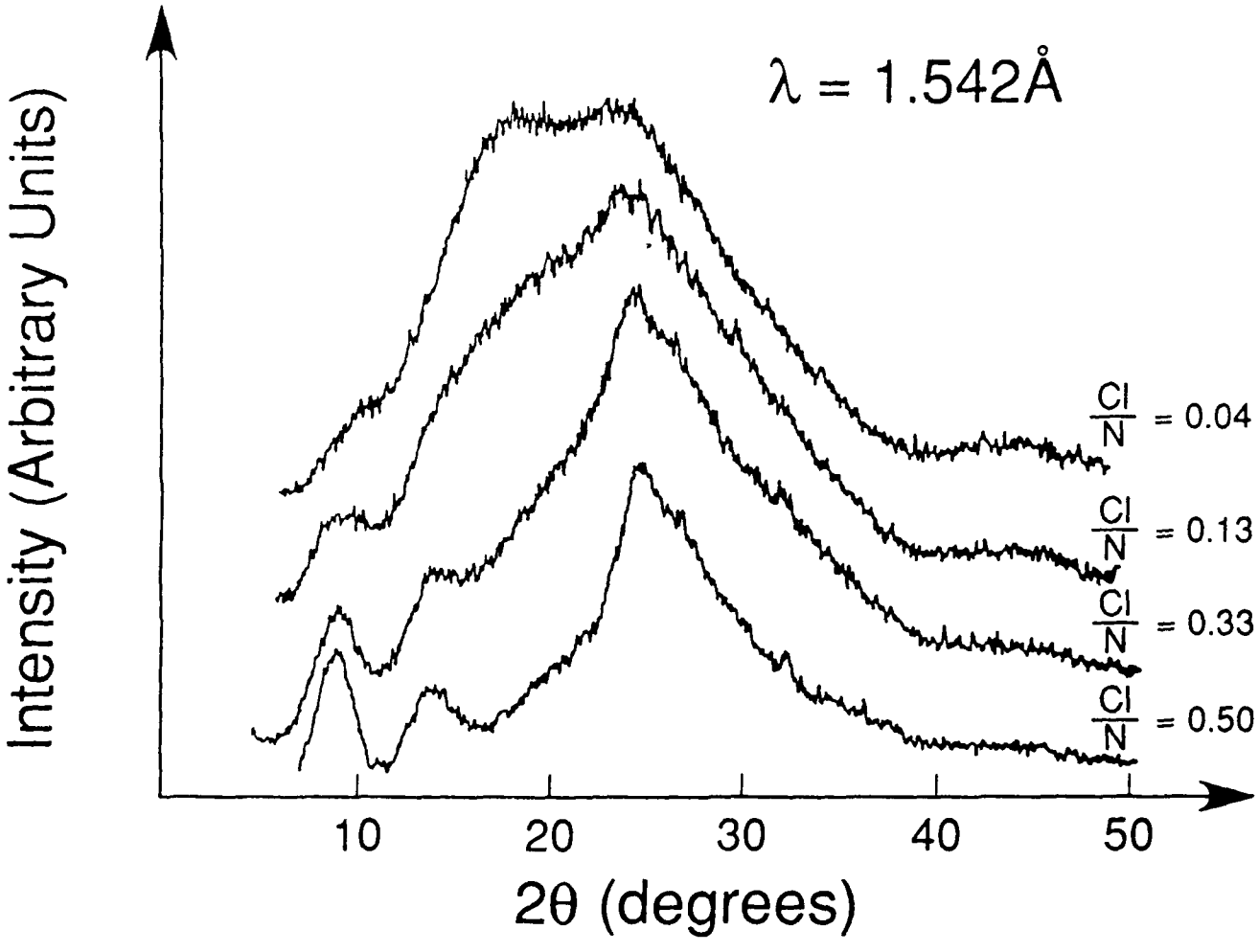

Jozefowicz et al. Figure 4

F2/11-541-2

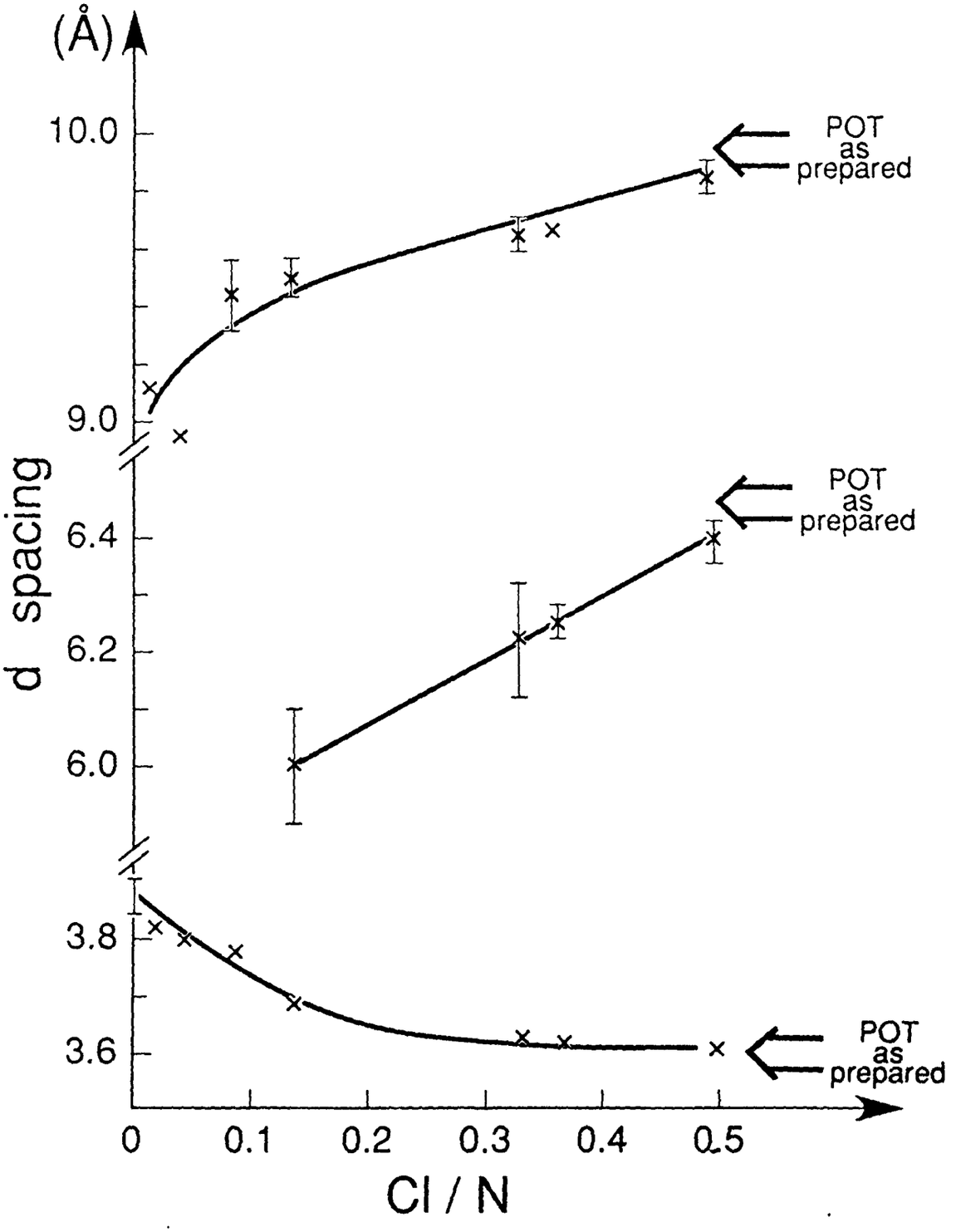

Jozefowicz et al. Figure 5

F2/11-54-1

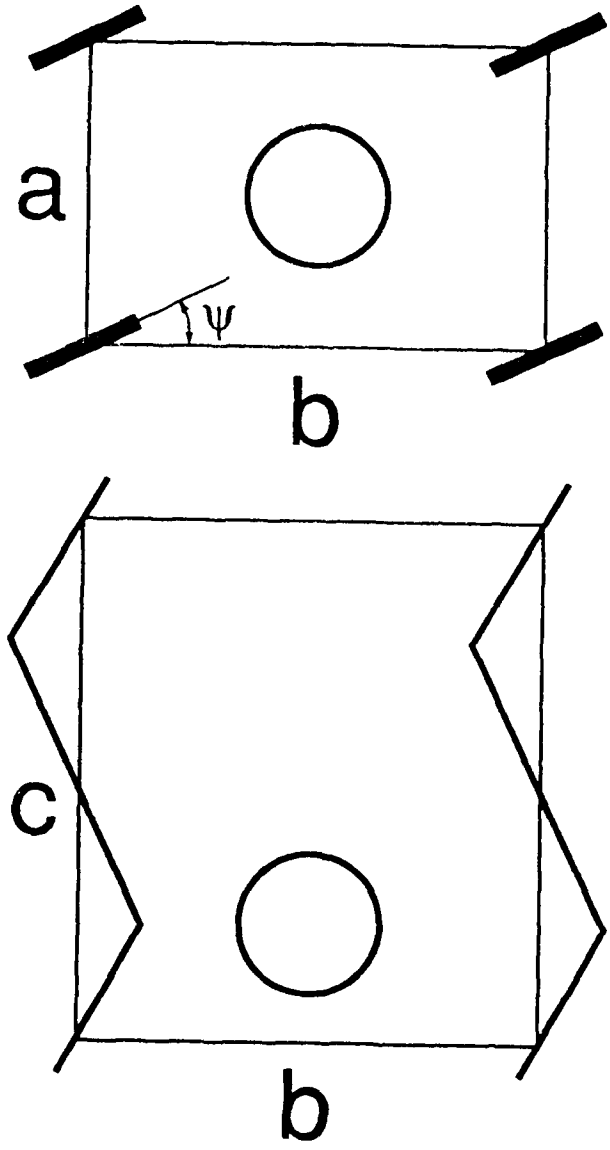

Jozefowicz et al. Figure 6

F2030-91-5